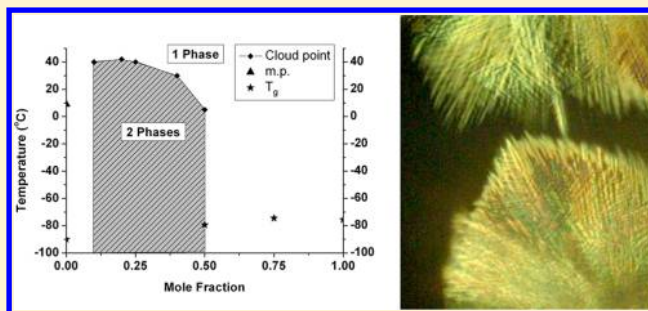


Ionic Liquid Mixtures—Variations in Physical Properties and Their Origins in Molecular Structure

Gary Annat,^{*,†} Maria Forsyth,[‡] and Douglas R. MacFarlane[†][†]School of Chemistry, Monash University, Wellington Rd, Victoria, Australia, 3800[‡]Institute for Frontier Materials, Deakin University, Burwood Hwy, Australia, 3125

S Supporting Information

ABSTRACT: In order to explore the various possible property trends in ionic liquid mixtures, five different ionic liquids were mixed with *N*-methyl-*N*-propylpyrrolidinium bis(trifluoromethylsulfonyl)amide ([C₃mpyr][NTf₂]), and the viscosities, excess molar volumes, ionic conductivities, and phase diagrams of the mixtures were determined over a range of temperatures. In a number of the mixtures the crystallization of both components was completely suppressed and no melting point was observable. Such mixtures of similar ionic liquids thus have potential for use in low-temperature applications by extending the liquid range to *T*_g. The molar conductivities and viscosities are described as approximating predictable or “simple” mixing behaviors, while excess molar volumes were found to show a variety of mixing and nonideal mixing effects. Mixture equations for viscosity and conductivity are discussed and analyzed. An immiscibility window was observed in the trihexyl(tetradecyl)phosphonium bis(trifluoromethylsulfonyl)amide ([P_{6,6,6,14}][NTf₂]) in the [C₃mpyr][NTf₂] system in the [C₃mpyr][NTf₂]-rich region. Unusual physical properties are exhibited by miscible compositions near the demixing line. These compositions are described as [P_{6,6,6,14}][NTf₂]-like, even up to 0.5 mol fraction of [C₃mpyr][NTf₂].



■ INTRODUCTION

Ionic liquids (ILs) have been identified as materials that can potentially replace volatile organic solvents in many processes to improve safety and reduce environmental impact due to their unique combination of properties.^{1,2} That is, ILs potentially offer a material with negligible volatility, electrochemical stability, thermal stability, and ionic conductivity, all accessible at or near ambient temperatures and pressures. A huge range of possible anions and cations generates many different possible ILs with varying properties to choose from. There have been, however, relatively few applications that have commercialized ILs,³ often due to an undesirably high viscosity (with a notable exception of tribological applications where viscosity may be a desirable feature). Adding other materials to ILs as diluents is seen as a possible method to alter their physical properties,⁴ as there are many molecular solvents that are readily available and whose properties have been extensively studied. Although molecular solvents can reduce the viscosity of an IL, the resulting mixture has an increased volatility and therefore lower thermal stability.⁵ On the other hand, mixing ILs with other ILs (IL–IL mixtures) is seen as a possible method to improve target properties of the IL while maintaining their favorable characteristics.

Due to the large number of possible ILs and therefore the extraordinarily large number of possible IL–IL mixtures, this is a broad and uncertain area of investigation. There have been several applications where ILs mixed with other ILs have shown

promising results, including gas solubilities,⁶ dye-sensitized solar cells,^{7–10} solvent reaction media,¹¹ and as a gas chromatography stationary phase.¹² There have also been some theoretical studies of IL–IL mixtures^{13–15} and an examination of the polar and nonpolar regions known to exist in ILs.¹⁶ There have been some limited measurements of the physical properties of IL–IL mixtures, notably melting behaviors,^{17,18} nanostructures,¹⁹ molecular association,²⁰ dielectric measurements,²¹ transport and volumetric properties,^{22–26} responses to solvatochromic probes,²⁷ and optical heterodyne-detected Raman-induced Kerr effect spectroscopy (OHD-RIKES).²⁸ Some studies have shown that the properties of IL–IL mixtures can be described by “simple” mixing behavior, that is, a linear trend of the property as a function of concentration between the two pure ILs.^{13,21} There have been some instances of improved properties above those of the individual ILs.^{6,22}

On the other hand, some mixtures of ILs become mutually immiscible (i.e., split into two phases at certain compositions and temperatures),²⁹ hence indicating that simple mixing is not ubiquitous in IL binaries. Reports of these systems have so far focused on their suitability for separating alkanes and alkenes,^{29–31} though demixing temperatures and compositions

Received: February 8, 2012

Revised: June 11, 2012

Published: July 3, 2012

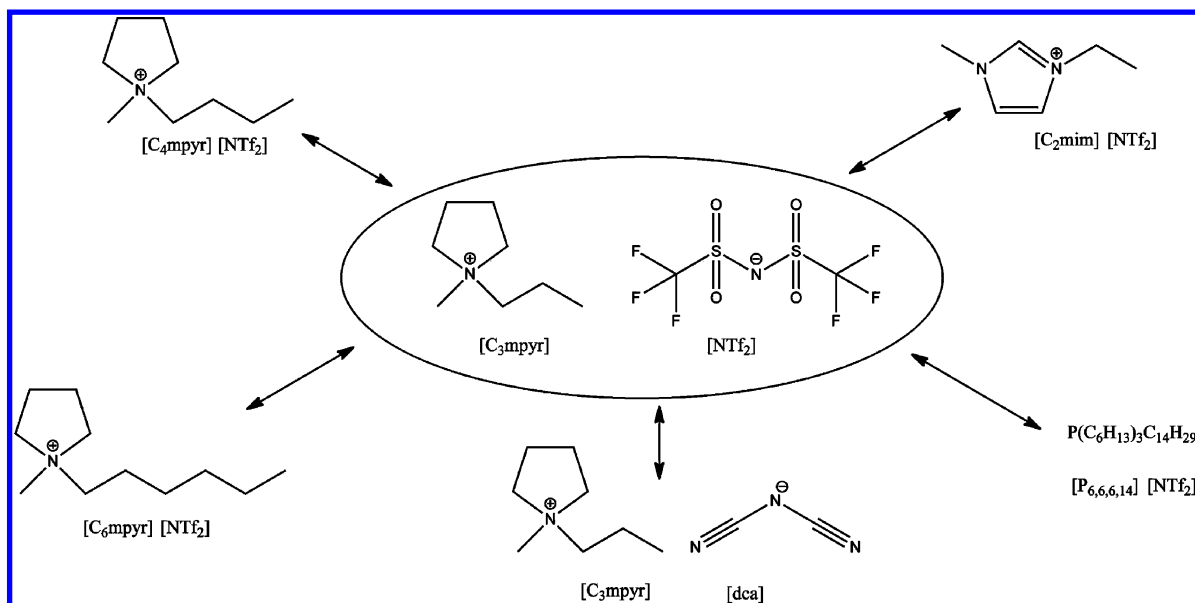


Figure 1. Structures and shorthand names of the ILs studied in this work.

have been reported for 1-ethyl-3-methylimidazolium bis-(trifluoromethylsulfonyl)amide ([C₂mim][NTf₂]) and *N*-ethylpyridinium bis(trifluoromethylsulfonyl)amide ([C₂py][NTf₂]) mixed with trihexyl(tetradecyl)phosphonium bis-(trifluoromethylsulfonyl)amide [P_{6,6,6,14}][NTf₂].^{29,30}

In order to probe further the appearance of simple versus more complex mixing behavior as a function of the type of ions present, this study examined the properties of systems with a common anion and different cations, as well as one system with a common cation but different anions. To make differences in IL–IL interactions more obvious, a common IL was chosen for all the mixture systems, *N*-methyl-*N*-propylpyrrolidinium bis(trifluoromethylsulfonyl)amide ([C₃mpyr][NTf₂]). The other ILs chosen for study were *N*-butyl-*N*-methylpyrrolidinium bis(trifluoromethylsulfonyl)amide ([C₄mpyr][NTf₂]), *N*-hexyl-*N*-methylpyrrolidinium bis(trifluoromethylsulfonyl)amide ([C₆mpyr][NTf₂]), [C₂mim][NTf₂], *N*-methyl-*N*-propylpyrrolidinium dicyanamide ([C₃mpyr][dca]), and [P_{6,6,6,14}][NTf₂] (see Figure 1). The viscosities, densities, phase diagrams, and ionic conductivities are reported for all systems at room temperature. There is particular attention paid to the [P_{6,6,6,14}][NTf₂] in [C₃mpyr][NTf₂] system due to an observed miscibility gap. The physical properties for this system are reported, which show significant deviation from normal mixing behavior approaching the demixing composition.

EXPERIMENTAL SECTION

All compounds containing the bis(trifluoromethylsulfonyl)amide anion ([NTf₂]), except for [P_{6,6,6,14}][NTf₂], were synthesized using a metathesis reaction described previously.³² *N*-Methyl-*N*-propylpyrrolidinium dicyanamide, [C₃mpyr][dca], was synthesized as described previously,³³ though bromide was used as a counterion rather than iodide in all syntheses, and imidazolium bromide was substituted for pyrrolidinium bromide in synthesis of [C₂mim][NTf₂]. [P_{6,6,6,14}][NTf₂], purchased from Cytec Industries Inc., was purified by washing with water and hexane and dried under vacuum until a constant pressure of 0.04 kPa was maintained for 3 h.

All ILs were checked for purity using NMR, mass spectrometry, and ion selective electrode determination of

halide content. Samples were dried under vacuum at 100 °C for at least 24 h. After drying, all compounds were stored in a drybox under nitrogen. Water content, measured using a Karl Fischer titration, was <10 ppm for all [NTf₂][−]-based ILs and =310 ppm for [C₃mpyr][dca]. Bromide content in all synthesized [NTf₂][−]-based ILs was <10 ppm. Mass spectrometry was measured using a Micromass Platform II ESI-MS, and all compounds showed only the parent ion peaks. ¹H NMR was measured on a Bruker DPX300.

Differential scanning calorimetry (DSC) experiments were conducted using a ThermalAnalysis DSC Q100, and data was analyzed using Universal Analysis 2000 V4.1D, Build 4.1.0.16 software. Samples were loaded into sample pans under nitrogen. Samples were cooled at 10 °C/min, held at temperature for 5 min, and then heated at 10 °C/min. All samples were analyzed at least three times, to determine material behavior and avoid sample and instrument artifacts.

Density was measured using an Anton Paar DMA5000 density meter, precise to ±0.0005 °C and ±0.000 001 g cm^{−3}. Viscosity was measured on an Anton Paar AMVn viscometer, which uses a falling ball technique. Data was analyzed using “Visiolab for AMVn” version 1.61.2440.

Ionic conductivities were determined by measuring their resistance and impedance as a function of frequency using electronic impedance spectroscopy (EIS). Measurements were made using a Solartron 1296 dielectric interface linked to a 1290 frequency response analyzer. Data was analyzed using Solartron impedance measurement software (v. 3.3.1). Samples were measured in a vial, with a custom-made glass plunger with two platinum wires protruding from the plunger into the sample acting as electrodes. This setup has been described previously.²³ Cell constants were determined using a 0.01 M KCl_(aq) solution. Typical reproducibility was found to be ~1%.

RESULTS

Phase Diagrams and Anomalous Liquid–Solid Behavior. DSC scans of the mixtures show complex phase transitions that can overlap each other, as demonstrated by the [C₃mpyr][dca] in [C₃mpyr][NTf₂] system shown in Figure 2.

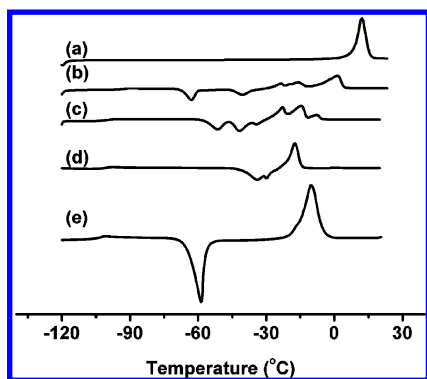


Figure 2. DSC traces of $[\text{C}_3\text{mpyr}][\text{dca}]$ in $[\text{C}_3\text{mpyr}][\text{NTf}_2]$ mixtures. Compositions are (a) 0, (b) 0.25, (c) 0.5, (d) 0.75, and (e) 1 mol fraction $[\text{C}_3\text{mpyr}][\text{dca}]$.

While pure $[\text{C}_3\text{mpyr}][\text{dca}]$ (Figure 2e) shows a single devitrification exotherm beginning at -65°C , all the mixtures show several devitrification exotherms, some of which overlap. This indicates that different devitrification processes are occurring at the same time. This could be the result of complex phase behavior or of the formation of different crystal phases in the sample matrix. The DSC trace for each mixture can be found in Figures S1–S22 in the Supporting Information.

Several of the mixtures appear to follow simple binary phase behavior (Figure 2), with depression of the melting points of each pure component and in some cases a eutectic transition being observed. Defining specific phase transitions was difficult due to the overlap of peaks as well as the indistinct transition from exothermic to endothermic peaks. In cases where a peak-onset temperature could not be determined, peak-maximum temperatures were used. For all figures, 0 mol fraction refers to pure $[\text{C}_3\text{mpyr}][\text{NTf}_2]$.

Figure 3a,b shows the phase diagrams for two different ILs mixed with $[\text{C}_3\text{mpyr}][\text{NTf}_2]$. Figure 3a is typical of a binary system with a eutectic transition. In this case the interpretation of the phase behavior is relatively classical; the addition of the second component lowers the melting point of the main component, A, and the line of melting points, more correctly described as the liquidus line, drops until it intersects the liquidus line of the other component. This intersection point defines the eutectic composition and temperature; in the case of Figure 3a at 0.75 mol fraction $[\text{C}_3\text{mpyr}][\text{dca}]$ and -27°C . Below the eutectic transition the sample is completely solid, consisting of a mixture of the two crystalline components. If

there is solid solubility of one of the components in the crystalline phase of the other, then the composition of these crystalline phases may not be that of the pure components. On warming through the eutectic transition at the eutectic composition, the sample completely melts. At other compositions, one of the crystalline components melts at the eutectic temperature, giving rise to the eutectic endotherm in the DSC. The remaining crystalline component continues to melt during continued warming until completion at the liquidus temperature, T_L . The eutectic transition is not observed in the $[\text{C}_3\text{mpyr}]/[\text{C}_4\text{mpyr}]$ binary of Figure 3b, indicating that the minor component is always difficult to crystallize; nonetheless, a eutectic at 0.5 mol fraction and at -25°C can be estimated. The 0.5 mol fraction mixture of $[\text{C}_4\text{mpyr}][\text{NTf}_2]$ in $[\text{C}_3\text{mpyr}][\text{NTf}_2]$ has been studied previously by Kunze et al.,¹⁷ who showed that the phase transitions for this mixture were dependent on the thermal history of the sample. The thermogram recorded in this study was almost identical to the trace reported by Kunze et al.¹⁷ under the same conditions. The additional peaks in Figure 3 labeled “endotherm” are probably eutectic and/or metastable phase melting.

The phase diagrams in Figure 4 show regions of the binary mixtures where no freezing/melting behavior is seen, indicating that the ability of the crystalline phases to nucleate and grow has been substantially quenched. In Figure 4a there is no freezing/melting transition associated with the 0.75 mol fraction $[\text{C}_6\text{mpyr}][\text{NTf}_2]$ mixture. Therefore, this mixture remains liquid (with increasing viscosity) all the way down to -85°C at which point it forms a glass (see inset). Materials that behave like this have been identified as potentially useful for low-temperature applications that require a liquid component.^{17,34} Figure 4b shows that two of the compositions tested for the $[\text{C}_2\text{mim}][\text{NTf}_2]$ in $[\text{C}_3\text{mpyr}][\text{NTf}_2]$ system also showed no crystalline phase in their phase diagram. It should be noted that the thermal history of the sample, DSC scanning conditions, and sample sizes are factors in determining crystallization behavior.³⁵ While no crystalline phase was observed in these studies, other techniques (e.g., annealing during scans, NMR analysis³⁶) could be employed to discover if crystalline phases can ever form in these mixtures.

Figure 5a shows the phase diagram for the $[\text{P}_{6,6,6,14}][\text{NTf}_2]$ in $[\text{C}_3\text{mpyr}][\text{NTf}_2]$ system and a highlighted section representing a section of immiscibility between 0.1 and 0.5 mol fraction $[\text{P}_{6,6,6,14}][\text{NTf}_2]$. The immiscibility was observed as a cloudy single phase that would split into two clear layers after a few

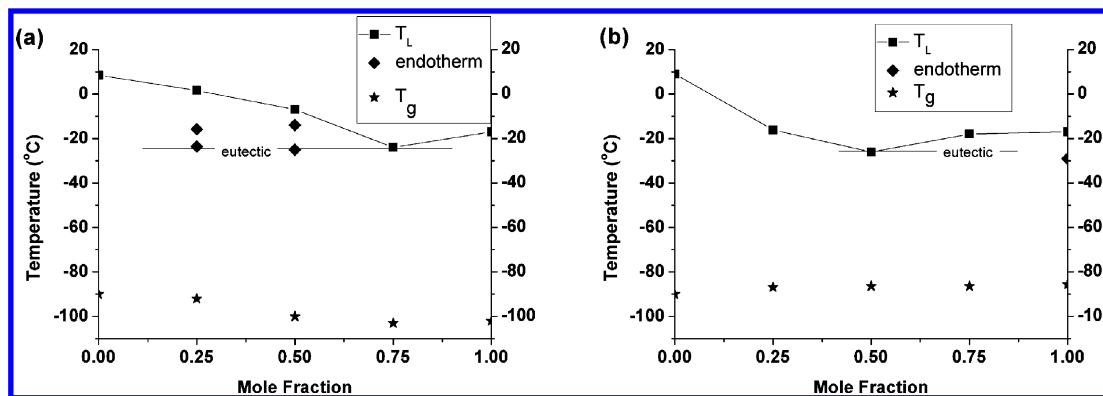


Figure 3. Phase diagrams for binary mixtures of $[\text{C}_3\text{mpyr}][\text{NTf}_2]$ and (a) $[\text{C}_3\text{mpyr}][\text{dca}]$ and (b) $[\text{C}_4\text{mpyr}][\text{NTf}_2]$ (T_L = liquidus temperature; T_g = glass transition).

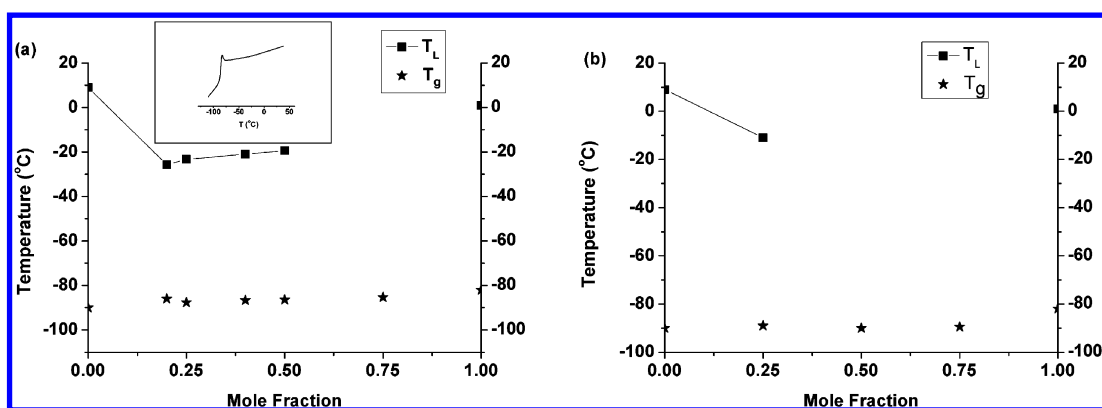


Figure 4. Phase diagrams of (a) $[C_6\text{mpyr}][NTf_2]$ in $[C_3\text{mpyr}][NTf_2]$ (inset: thermogram of 0.75 mol fraction $[C_6\text{mpyr}][NTf_2]$ showing only a T_g) and (b) $[C_2\text{mim}][NTf_2]$ in $[C_3\text{mpyr}][NTf_2]$.

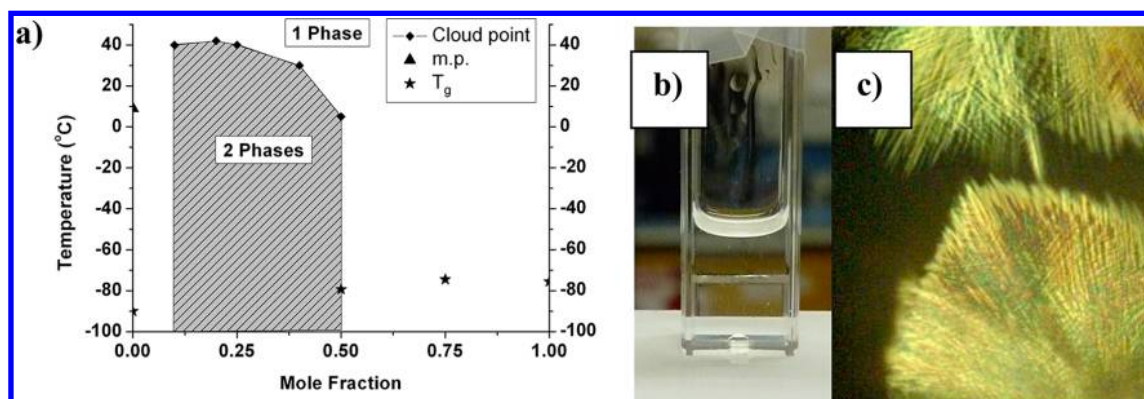


Figure 5. (a) Phase diagram for $[P_{6,6,6,14}][NTf_2]$ in $[C_3\text{mpyr}][NTf_2]$ mixtures; an immiscibility gap is highlighted. (b) Picture of the two phase system. (c) Optical micrograph of crystal growth below UCT.

minutes. Mixtures between 0.1 and 0.5 mol fraction $[P_{6,6,6,14}][NTf_2]$ exhibited an upper critical solution temperature (UCST), above which solutions would form one clear phase at any composition. Figure 5c shows the appearance of crystals growing in the 0.5 mol fraction mixture after cooling to 0 °C from the clear, single phase liquid mixture at room temperature. This represents a melting point depression with respect to pure $[C_3\text{mpyr}][NTf_2]$, plus any supercooling, of only 9 °C; hence, it was surprising to see such ready crystallization at this temperature. The crystals grew slowly due to the high viscosity of the liquid matrix. After an hour, it was apparent that the crystals had stopped growing, with about one-third of the sample crystallized. Upon reheating, the crystals melted at approximately 8 °C; the resultant liquid mixture was single phase. This is only a 1 °C melting point depression with respect to pure $[C_3\text{mpyr}][NTf_2]$; in the other mixtures studied here (Figure 3) at 0.5 mol fraction, a melting point depression of at least 15 °C is typical. Hence, it appears that the implied liquidus line is very flat in this system, potentially as a result of the proximity to the liquid–liquid demixing line. In fact, if the demixing temperature at this composition was between 8 and 0 °C, the phase separation would produce a $[C_3\text{mpyr}][NTf_2]$ -rich phase that would be below its equilibrium liquidus point and hence would slowly freeze. The removal of liquid $[C_3\text{mpyr}][NTf_2]$ from the liquid–liquid equilibrium would draw further $[C_3\text{mpyr}][NTf_2]$ from the other phase. Hence, most of the $[C_3\text{mpyr}][NTf_2]$ in the sample would ultimately freeze. The observations made here are consistent with this hypothesis but, of course, do not prove it.

Excess Molar Volume (V^E). Excess molar volume (V^E) is defined as the difference in measured molar volume of a mixture from the expected molar volume. The expected molar volume is determined from the sample density and the weighted average of the molar volume of each pure IL. Therefore, V^E is determined by the following equation

$$V^E = \frac{xM_{w(a)} + (1-x)M_{w(b)}}{\rho} - (xV_{M(a)} + (1-x)V_{M(b)}) \quad (1)$$

where x is the mole fraction, M_w is the molecular weight, ρ is the density, V_M is the molar volume and a and b denote different ILs. A larger volume than expected, therefore, is defined as a positive excess volume, and a smaller volume is a negative excess. Density and V^E for each system as a function of composition and temperature can be seen in Figures S23–S32 in the Supporting Information.

Figure 6 shows all the calculated V^E s for the mixtures at 20 °C. Data for other temperatures are available in the Supporting Information. It appears the V^E values for three of the mixtures are within error of ideal mixing with respect to density (i.e., $V^E = 0 \text{ cm}^3 \text{ mol}^{-1}$). V^E for the $[C_3\text{mpyr}][dca]$ in $[C_3\text{mpyr}][NTf_2]$ system is asymmetric with respect to the 0.5 mol fraction composition, as has been seen before in other types of mixtures,^{25,37} though entirely symmetric V^E s have also been observed.²⁴ The magnitude of these V^E s is comparable to those measured in other systems,^{24,25} but the V^E s for the $[P_{6,6,6,14}][NTf_2]$ in $[C_3\text{mpyr}][NTf_2]$ system are significantly larger.

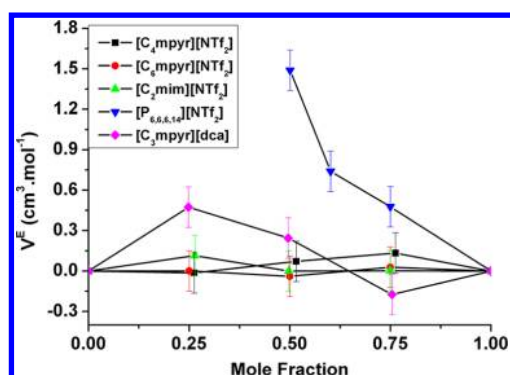


Figure 6. Excess molar volumes (V^E) for all ILs in $[C_3\text{mpyr}][\text{NTf}_2]$ (tie lines are a visual aid only).

Viscosity. Viscosities of binary mixtures vary in their behavior, and several different equations exist to describe the different forms. The following equation has been found to be best for describing how viscosity changes with composition for IL–IL mixtures^{21,38}

$$\log \eta = x \log \eta_a + (1 - x) \log \eta_b \quad (2)$$

where x is the mole fraction of compound a, η is the viscosity of the mixture, and η_a and η_b are the viscosities of pure compounds a and b, respectively. Figure 7 shows the data for

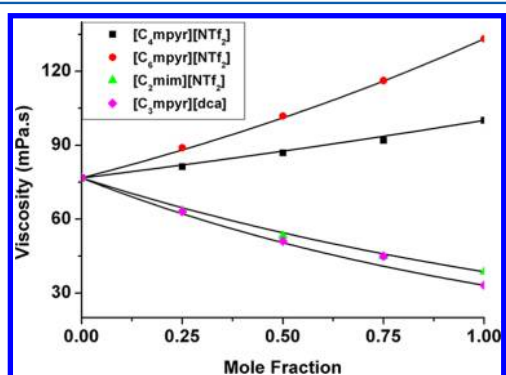


Figure 7. Viscosities of several mixtures at 20 °C (uncertainties are smaller than the size of the data points). Solid lines are as predicted from eq 2. Some data used from ref 23. (Data for other temperatures are available in the Supporting Information.)

four of the studied mixture systems at 20 °C and the calculated viscosities for each system calculated from eq 2. Data for other temperatures are available in the Supporting Information.

Previous studies of molecular solvents and an IL⁴ has also shown viscosity to be adequately described by the following equation

$$\eta = \eta_s \exp\left(\frac{-x_{cs}}{a}\right) \quad (3)$$

where η is the viscosity of the mixture, η_s is the viscosity of pure IL, x_{cs} is the concentration of the countercation, and a is an unknown fitting parameter. In fact, eq 3 is the same as eq 2, where $1/a = -\log(\eta_b/\eta_a)$ and hence this form of the equation is able to model a wide range of mixture types.

The $[P_{6,6,6,14}][\text{NTf}_2]$ in $[C_3\text{mpyr}][\text{NTf}_2]$ system, shown in Figure 8, showed a significant deviation from any type of simple mixing behavior. This figure shows that the addition of $[C_3\text{mpyr}][\text{NTf}_2]$ to $[P_{6,6,6,14}][\text{NTf}_2]$ only moderately reduces

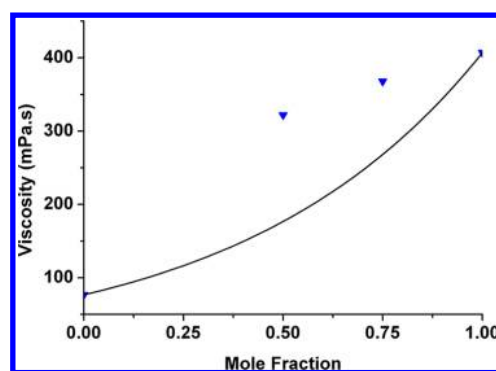


Figure 8. Measured viscosities of $[P_{6,6,6,14}][\text{NTf}_2]$ in $[C_3\text{mpyr}][\text{NTf}_2]$ mixtures; the solid line was calculated from eq 2.

the viscosity from that of the pure $[P_{6,6,6,14}][\text{NTf}_2]$. It is likely that the long alkyl chains of the $[P_{6,6,6,14}]^+$ cation form nonpolar domains in the matrix and that the addition of $[C_3\text{mpyr}]^+$ fails to alter these domains significantly. It would be anticipated that wide angle X-ray scanning studies (such those of Triolo et al.¹⁶) of this mixture system would find little difference between the nonpolar domain sizes in the pure $[P_{6,6,6,14}][\text{NTf}_2]$ and those in the mixtures.

Conductivity. Molar conductivities are calculated from ionic conductivities, measured by impedance spectroscopy, and a molar concentration calculated from the measured density and the mole fraction as shown in Figure 8. Ionic conductivities for all mixtures are in Figures S38–S42 in the Supporting Information. As with the viscosity data, it is not unusual for these systems to have nonlinear or complex properties with mixing, although the $[C_2\text{mim}][\text{NTf}_2]$ in $[C_3\text{mpyr}][\text{NTf}_2]$ system, on the other hand, appears to change very linearly with composition. A variation of eq 2 has been used in Figure 9 to model molar conductivity, where Λ is used in place of η , eq 4, and it appears to do so satisfactorily.

$$\log \Lambda = x \log \Lambda_a + (1 - x) \log \Lambda_b \quad (4)$$

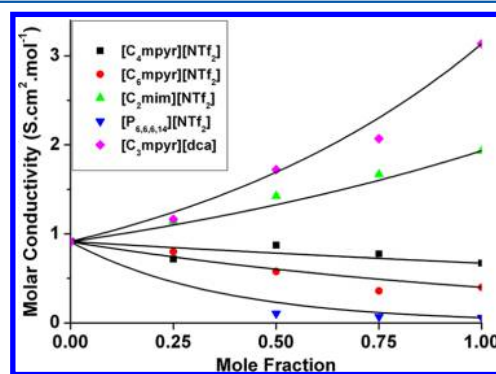


Figure 9. Molar conductivities of IL–IL mixtures at 20 °C as a function of IL composition in $[C_3\text{mpyr}][\text{NTf}_2]$ (uncertainties are smaller than the size of data points); lines are as predicted by eq 4. Some data used from ref 23.

As with the other measurements, it is obvious that the $[P_{6,6,6,14}][\text{NTf}_2]$ in $[C_3\text{mpyr}][\text{NTf}_2]$ system is different from the other systems. The molar conductivity of the mixtures changes very little from the pure $[P_{6,6,6,14}][\text{NTf}_2]$, even with up to 0.5 mol fraction $[C_3\text{mpyr}][\text{NTf}_2]$.

Ionicity of IL–IL Mixtures through Walden Plot Analysis. The ILs $[\text{C}_3\text{mpyr}][\text{NTf}_2]$, $[\text{C}_2\text{mim}][\text{NTf}_2]$, and $[\text{C}_3\text{mpyr}][\text{dca}]$ are all fluid and highly conducting. Previous analysis of the pure ILs shows they have roughly the same degree of ionicity.³⁹ On the Walden plot (Figure 10), these

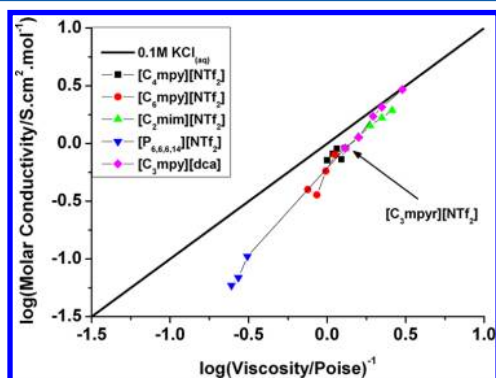


Figure 10. Walden plot of IL–IL mixtures, with tie lines through each mixture and pure $[\text{C}_3\text{mpyr}][\text{NTf}_2]$ indicated by the arrow.

mixtures show a gradual, linear change in properties from one IL to the other. The difference between $\log \Lambda$ and $\log(\eta^{-1})$, ΔW , is interpreted as a reflection of the degree of ion association in the medium.⁴⁰ The Walden plot is, however, also affected by the radius of the ions in solution.³⁹ The substitution of the Stokes–Einstein relation into the Nernst–Einstein relation yields a modified form of the Walden rule

$$\Lambda = \frac{N_A e^2}{6\pi} \eta^{-1} \left(\frac{1}{r^+} + \frac{1}{r^-} \right) \quad (5)$$

where N_A is Avogadro's constant, e is the charge on an electron (coulombs), and r^+ and r^- denote the effective radii of the cation and anion, respectively. This allows calculation of a value for ΔW adjusted for the ion size. Figures S43–S48 in the Supporting Information show the behavior of this adjusted ΔW in the IL–IL mixtures as a function of mole fraction and as a function of temperature. The trends in composition show relatively minor changes at 20 °C. These figures also show that ΔW , and therefore ion association, increase very slightly with increasing temperature.

DISCUSSION

It is clear from the data presented that the physical properties exhibited by the various mixtures depend on the ILs used, even in this work, where one IL was kept constant over all the systems. We categorize our discussion below on the basis of the structure of the second component.

Pyrrolidinium IL Mixtures. $[\text{C}_4\text{mpyr}][\text{NTf}_2]$ and $[\text{C}_6\text{mpyr}][\text{NTf}_2]$ were chosen for archetypical IL–IL mixtures with only subtle structural differences. These two ILs also have very similar physical properties to $[\text{C}_3\text{mpyr}][\text{NTf}_2]$, with respect to density, viscosity, and conductivity. Given that these cations have a very similar shape and only a small difference in size, it would be expected they would interact with $[\text{C}_3\text{mpyr}]^+$ cations much as one $[\text{C}_3\text{mpyr}]^+$ would interact with another. Phase diagrams of the two mixture systems showed little change in T_g for all mixtures, but the 0.75 mol fraction $[\text{C}_6\text{mpyr}][\text{NTf}_2]$ mixture showed no melting point. This may be due to the supercooling nature of the ILs around this composition.

Both pyrrolidinium mixtures exhibited simple mixing behaviors for viscosity and almost negligible V^E s. This suggests that the $[\text{C}_6\text{mpyr}]^+$ and $[\text{C}_4\text{mpyr}]^+$ cations have little effect on how the ions arrange and move in the liquid state. The change in molar conductivity with composition for these systems was not linear, though the changes were minor due to the similar conductivities of the three ILs.

Hydrophilic vs Hydrophobic Anions. $[\text{C}_3\text{mpyr}][\text{dca}]$ was chosen for this work, as it has the same cation but a very different anion. The $[\text{dca}]^-$ anion is smaller, lighter, and very hydrophilic, contrasting the large, heavy, and hydrophobic $[\text{NTf}_2]^-$ anion. DSC analysis of the mixtures showed that several different crystalline phases devitrified and melted around the same temperature. Supercooling of the liquid phase and the presence of several different crystalline phases in the solid state means this system has a complex solid phase.

This system shows a high V^E for the majority $[\text{NTf}_2]^-$ mixture and a low (but almost negligible) V^E in the majority $[\text{dca}]^-$ mixture. This would indicate that the $[\text{dca}]^-$ anion hinders efficient packing in a $[\text{C}_3\text{mpyr}][\text{NTf}_2]$ -majority material but that $[\text{NTf}_2]^-$ promotes more efficient packing in a $[\text{C}_3\text{mpyr}][\text{dca}]$ -majority material. Though the viscosity data followed simple mixing, the molar conductivity for this system did not display a steady change between the two ILs.

Aromatic- and Phosphonium-Based Cations. To investigate very different cations in IL–IL mixtures, an aromatic-based IL, $[\text{C}_2\text{mim}][\text{NTf}_2]$, and a tetraalkylphosphonium based IL, $[\text{P}_{6,6,6,14}][\text{NTf}_2]$, were chosen. The $[\text{C}_2\text{mim}][\text{NTf}_2]$ in $[\text{C}_3\text{mpyr}][\text{NTf}_2]$ showed very little variation from simple mixing, especially for molar conductivity and viscosity measurements. The V^E data did vary slightly and suggested that $[\text{C}_2\text{mim}][\text{NTf}_2]$ added to $[\text{C}_3\text{mpyr}][\text{NTf}_2]$ induces slightly inefficient packing. The phase diagram for this system showed that two of the three mixtures measured failed to crystallize at all in the DSC. Since these materials have a relatively low viscosity at room temperature, these mixtures may be useful as electrolytes or as a liquid medium at low temperatures.

$[\text{P}_{6,6,6,14}][\text{NTf}_2]$ mixed with $[\text{C}_3\text{mpyr}][\text{NTf}_2]$ also produced mixtures that failed to crystallize. These mixtures already have a high viscosity at room temperature, so at lower temperatures they would likely have a prohibitively high viscosity for many applications. All the physical properties measured for this system can be described as having similar properties to the pure $[\text{P}_{6,6,6,14}][\text{NTf}_2]$. The viscosities of the mixtures in this system illustrate particularly well that the physical properties did not trend in a simple fashion from one pure IL to the other. Instead, they hovered closely to that of the pure $[\text{P}_{6,6,6,14}][\text{NTf}_2]$ until the immiscibility gap. It is for this reason, and influenced by previous studies,^{14,16,41,42} that the domains formed by the alkyl chains in the pure $[\text{P}_{6,6,6,14}][\text{NTf}_2]$ are thought to be relatively unaffected by the addition of $[\text{C}_3\text{mpyr}][\text{NTf}_2]$ and that these domains dictate the physical properties of the mixtures. It would be reasonably expected that mixtures of $[\text{P}_{6,6,6,14}][\text{NTf}_2]$ with many other ILs with small alkyl chains (e.g., $[\text{C}_2\text{mim}][\text{NTf}_2]$ ²⁹) would have similar properties.

Immiscibility. The immiscibility gap in the $[\text{P}_{6,6,6,14}][\text{NTf}_2]$ in $[\text{C}_3\text{mpyr}][\text{NTf}_2]$ system in Figure 5 shows an upper critical temperature limit just above room temperature for $[\text{C}_3\text{mpyr}][\text{NTf}_2]$ -rich compositions. The critical demixing temperature for the 1:1 mixture in this system was difficult to determine, due to the high viscosity. Even in the other concentrations where the UCST was 40 °C, the cloudiness would take over 10

s to appear or disappear and over 30 min for the two phases to separate. When the 1:1 mixture was cooled, it would take a long time for cloudiness to appear, even though the sample was much colder than the UCST. Immiscibility regions in $[P_{6,6,6,14}]^+$ -based ILs have been described previously,²⁹ though it is interesting to note that others have found immiscibility gaps in the $[P_{6,6,6,14}][NTf_2]$ -rich region for several compounds, unlike this study.

CONCLUSIONS

Binary ionic liquid in ionic liquid mixtures were analyzed as a function of composition and temperature, measuring phase behavior, viscosity, density, and molar conductivity. In all five mixtures, $[C_3mpyr][NTf_2]$ was used as one of the ILs in each mixture.

All systems showed melting point depression of the components. Some mixtures of $[C_6mpyr][NTf_2]$ and $[C_2mim][NTf_2]$ with $[C_3mpyr][NTf_2]$ produced materials that showed no crystallization tendency and hence became glass-forming. All mixtures of $[P_{6,6,6,14}][NTf_2]$ with $[C_3mpyr][NTf_2]$ were glass-forming. It appears, therefore, that mixing of cations, in some cases of relatively similar structure, provides a means of lowering melting points and considerably extending the low temperature liquid range.

Most of the physical properties for the IL–IL mixtures exhibited simple mixing behavior (with occasional scatter). The $[P_{6,6,6,14}][NTf_2]$ in $[C_3mpyr][NTf_2]$ system did not follow simple mixing for any of the measured properties. V^E for this system was the highest measured, and the viscosity and molar conductivity data showed the mixtures could be described as being more $[P_{6,6,6,14}][NTf_2]$ -like than a mixture of the two ILs. This was attributed to the large alkyl chains on the phosphonium cation likely forming nanoscale nonpolar domains, as reported elsewhere, which remain unchanged in the mixtures, even up to a 1:1 mixture with $[C_3mpyr][NTf_2]$. An immiscibility gap was also found for the $[P_{6,6,6,14}][NTf_2]$ in $[C_3mpyr][NTf_2]$ system, exhibiting an upper critical temperature. This is the first report of physical properties (such as viscosity and density) of a partially immiscible ionic liquid in ionic liquid system.

ASSOCIATED CONTENT

Supporting Information

Densities, excess molar volumes, viscosities, ionic conductivities, DSC traces, and ΔW values for the compounds and mixtures studied in this work. This material is available free of charge via the Internet at <http://pubs.acs.org>.

AUTHOR INFORMATION

Corresponding Author

*E-mail: garyjannat@gmail.com.

Notes

The authors declare no competing financial interest.

ACKNOWLEDGMENTS

The authors are grateful for funding from the Australian Research Council for Discovery Project funding and for D.R.M.'s Federation Fellowship. The authors would also like to acknowledge Dr. B. Clare and Dr. K. Johansson for synthesizing and purifying the compounds used in this study.

REFERENCES

- (1) Seddon, K. R. *J. Chem. Technol. Biotechnol.* **1997**, *68*, 351.
- (2) Welton, T. *Chem. Rev.* **1999**, *99*, 2071.
- (3) Freemantle, M. (Ed.) *An Introduction to Ionic Liquids*; RSC Publishing: London, 2010.
- (4) Seddon, K. R.; Stark, A.; Torres, M.-J. *Pure Appl. Chem.* **2000**, *72*, 2275.
- (5) Nakata, Y.; Kohara, K.; Matsumoto, K.; Hagiwara, R. *J. Chem. Eng. Data* **2011**, *56*, 1840.
- (6) Finotello, A.; Bara Jason, E.; Narayan, S.; Camper, D.; Noble Richard, D. *J. Phys. Chem. B* **2008**, *112*, 2335.
- (7) Zistler, M.; Wachter, P.; Schreiner, C.; Fleischmann, M.; Gerhard, D.; Wasserscheid, P.; Hinsch, A.; Gores, H. J. *J. Electrochem. Soc.* **2007**, *154*, B925.
- (8) Wang, P.; Zakeeruddin, S. M.; Humphry-Baker, R.; Graetzel, M. *Chem. Mater.* **2004**, *16*, 2694.
- (9) Hao, F.; Lin, H.; Liu, Y.; Yang, G.; Wang, G.; Li, J. *Electrochim. Acta* **2011**, *56*, 5605.
- (10) Hao, F.; Lin, H.; Liu, Y.; Li, J. *J. Phys. Chem. Chem. Phys.* **2011**, *13*, 6416.
- (11) Khosropour, A. R.; Mohammadpoor-Baltork, I.; Kiani, F. C. R. *Chim.* **2011**, *14*, 441.
- (12) Baltazar, Q. Q.; Leininger, S. K.; Anderson, J. L. *J. Chromatogr., A* **2008**, *1182*, 119.
- (13) Shimizu, K.; Tariq, M.; Rebelo, L. P. N.; Lopes, J. N. C. *J. Mol. Liq.* **2010**, *153*, 52.
- (14) Canongia Lopes, J. N. A.; Padua, A. A. H. *J. Phys. Chem. B* **2006**, *110*, 3330.
- (15) Bruessel, M.; Brehm, M.; Voigt, T.; Kirchner, B. *Phys. Chem. Chem. Phys.* **2011**, *13*, 13617.
- (16) Triolo, A.; Russina, O.; Bleif, H.-J.; Di Cola, E. *J. Phys. Chem. B* **2007**, *111*, 4641.
- (17) Kunze, M.; Jeong, S.; Paillard, E.; Winter, M.; Passerini, S. *J. Phys. Chem. C* **2010**, *114*, 12364.
- (18) Baltazar, P. M.; Best, A. S.; MacFarlane, D. R.; Forsyth, M. *ChemPhysChem* **2011**, *12*, 823.
- (19) Greaves, T. L.; Kennedy, D. F.; Kirby, N.; Drummond, C. J. *Phys. Chem. Chem. Phys.* **2011**, *13*, 13501.
- (20) Llovel, F.; Valente, E.; Vilaseca, O.; Vega, L. F. *J. Phys. Chem. B* **2011**, *115*, 4387.
- (21) Stoppa, A.; Buchner, R.; Heftner, G. *J. Mol. Liq.* **2010**, *153*, 46.
- (22) Every, H.; Bishop, A. G.; Forsyth, M.; MacFarlane, D. R. *Electrochim. Acta* **2000**, *45*, 1279.
- (23) Annat, G.; MacFarlane, D. R.; Forsyth, M. *J. Phys. Chem. B* **2007**, *111*, 9018.
- (24) Lopes, J. N. C.; Cordeiro, T. C.; Esperanca, J. M. S. S.; Guedes, H. J. R.; Huq, S.; Rebelo, L. P. N.; Seddon, K. R. *J. Phys. Chem. B* **2005**, *109*, 3519.
- (25) Navia, P.; Troncoso, J.; Romani, L. *J. Chem. Eng. Data* **2007**, *52*, 1369.
- (26) Castiglione, F.; Raos, G.; Battista Appetecchi, G.; Montanino, M.; Passerini, S.; Moreno, M.; Famulari, A.; Mele, A. *Phys. Chem. Chem. Phys.* **2010**, *12*, 1784.
- (27) Fletcher, K. A.; Baker, S. N.; Baker, G. A.; Pandey, S. *New J. Chem.* **2003**, *27*, 1706.
- (28) Xiao, D.; Rajian, J. R.; Li, S.; Bartsch, R. A.; Quitevis, E. L. *J. Phys. Chem. B* **2006**, *110*, 16174.
- (29) Arce, A.; Earle, M. J.; Katdare, S. P.; Rodriguez, H.; Seddon, K. R. *Chem. Commun.* **2006**, 2548.
- (30) Arce, A.; Earle, M. J.; Katdare, S. P.; Rodriguez, H.; Seddon, K. R. *Fluid Phase Equilib.* **2007**, *261*, 427.
- (31) Arce, A.; Earle, M. J.; Katdare, S. P.; Rodriguez, H.; Seddon, K. R. *Phys. Chem. Chem. Phys.* **2008**, *10*, 2538.
- (32) Macfarlane, D. R.; Meakin, P.; Sun, J.; Amini, N.; Forsyth, M. *J. Phys. Chem. B* **1999**, *103*, 4164.
- (33) Macfarlane, D. R.; Golding, J.; Forsyth, S.; Forsyth, M.; Deacon, G. B. *Chem. Commun.* **2001**, 1430.
- (34) Appetecchi, G. B.; Montanino, M.; Carewska, M.; Alessandrini, F.; Passerini, S. *Adv. Sci. Technol. (Stafa-Zuerich, Switz.)* **2010**, *72*, 315.

- (35) Henderson, W. A.; Herstedt, M.; Young, V. G., Jr.; Passerini, S.; De Long, H. C.; Trulove, P. C. *Inorg. Chem.* **2006**, *45*, 1412.
- (36) Madsen, L. A. *Macromolecules* **2006**, *39*, 1483.
- (37) Wang, J.; Tian, Y.; Zhao, Y.; Zhuo, K. *Green Chem.* **2003**, *5*, 618.
- (38) Navia, P.; Troncoso, J.; Romani, L. *J. Solution Chem.* **2008**, *37*, 677.
- (39) MacFarlane, D. R.; Forsyth, M.; Izgorodina, E. I.; Abbott, A. P.; Annat, G.; Fraser, K. *Phys. Chem. Chem. Phys.* **2009**, *11*, 4962.
- (40) Xu, W.; Cooper, E. I.; Angell, C. A. *J. Phys. Chem. B* **2003**, *107*, 6170.
- (41) Lopes, J. N. C.; Gomes, M. F. C.; Padua, A. A. H. *J. Phys. Chem. B* **2006**, *110*, 16816.
- (42) Gontrani, L.; Russina, O.; Lo Celso, F.; Caminiti, R.; Annat, G.; Triolo, A. *J. Phys. Chem. B* **2009**, *113*, 9235.